THERMOELECTRIC POWER AND RESISTIVITY OF COPPER-NICKEL ALLOYS

Thesis for the Degree of M. S. MICHIGAN STATE UNIVERSITY
Robert Allen Wolf
1963

THESIS

MICHIGAN STATE UNIVERSITY LIBRARIES

LIBRARY

Michigan State

University

PLACE IN RETURN BOX to remove this checkout from your record. TO AVOID FINES return on or before date due. MAY BE RECALLED with earlier due date if requested.

DATE DUE	DATE DUE	DATE DUE
208010		

11/00 c/CIRC/DateDue.p65-p.14

THERMOELECTRIC POWER AND RESISTIVITY OF COPPER-NICKEL ALLOYS

bу

Robert Allen Wolf

A THESIS

Submitted to
Michigan State University
in partial fulfillment of the requirements
for the degree of

MASTER OF SCIENCE

Department of Physics and Astronomy College of Natural Science ABSTRACT

The purpose of this program was (1) to obtain information about the Fermi surfaces of copper-nickel alloys through a study of the phonon drag contribution to the thermopower and (2) to study the dependence of the resistivity of copper-nickel alloys on temperature and concentration.

Two wires about one meter long by 0.02 centimeter in diameter were prepared for each of four alloys (0%, 0.85 wt. % Ni, 3.45 wt. % Ni, and 17.10 wt. % Ni). One of the wires, the thermoelectric voltage sample, was used as part of a Lead-alloy thermocouple with the cold junction in liquid nitrogen or helium and the hot junction in a copper block of known temperature. The other wire, the resistivity sample, was wound on a quartz rod, annealed, and placed in a cavity in the same copper block.

The thermoelectric voltage and resistivity of each of the four alloys were measured from 4.2 to 300° K. From these data, plots were made of (1) thermopower versus temperature; (2) resistivity versus temperature; (3) characteristic temperature, $\theta_{\rm R}$, versus temperature; (4) $\log(\rho-\rho_{\rm O})$ versus \log temperature; and (5) thermopower at 280° K versus resistivity⁻¹ at 280° K.

negative diffusion thermopowers and only that of the lowest concentration sample (0.85% nickel) had a positive phonon drag component. The absence of the expected phonon drag thermopower peaks in the other alloys, along with the relatively high resistivities of the alloys, are in agreement with other experimental evidence suggesting that 3d-band vacancies exist in copper-nickel alloys containing as little as 3% nickel.

ACKNOWLEDGMENTS

The author wishes to thank Dr. Peter A. Schroeder for suggesting this problem and for his assistance and encouragement throughout the course of the investigation.

The author is grateful to the National Science Foundation for their support of this program.

TABLE OF CONTENTS

Chapter		Page
I.	INTRODUCTION	1
II.	THEORY	2
	Thermoelectric Power Diffusion thermopower Phonon drag contribution to thermopower Electrical Resistivity Characteristic temperature, Θ_R Temperature dependence of resistivity	
III.	EXPERIMENTAL PROCEDURE	12
	Production of Alloy Samples Production of alloys Production of wires Construction of Cryostat Design of sample holder Wiring of sample holder Measurement of Thermoelectric voltage and resistivity Design of measuring circuit Procedure used in making measurements	
IV.	RESULTS	21
	Thermopower Electrical Resistivity Characteristic Temperature, Θ_{R} Temperature dependence of resistivity	
٧.	ANALYSIS OF RESULTS	35
	Thermopower Discussion of "absolute" and "measured" thermopower Summary of the Schroeder and Henry coppedinc results Expected relation between copper-nickel and copper-zinc results Discussion of copper-nickel thermopower results Resistivity	er-
VI.	CONCLUSIONS	52

LIST OF FIGURES

Figure	No.	Page
1.	Normal phonon-electron interaction (schematic).	8
2.	Umklapp phonon-electron interaction (schematic).	8
3.	Cryostat.	15
4.	Copper Block.	16
5.	Electrical circuit.	21
6.	Thermopower of copper-nickel alloys.	25
7.	Characteristic temperature, $\boldsymbol{\theta}_{R},$ of coppernickel alloys.	27
8.	Ideal resistivity of copper-nickel alloys.	23
9.	$\log (\rho - \rho_0)$ versus $\log T$ for copper-nickel alloys.	29
10.	Thermopower (280°K) versus resistivity ⁻¹ (280°K) for copper-nickel alloys.	3 4
11.	Schematic drawing of thermopower experiment	.36
12.	Thermopower of copper-zinc alloys.	<u>3</u> 8
13.	Fermi surface which has pulled away from the Brillouin Zone. (Schematic)	41
14.	Saturation magnetic moment, σ , and Curie temperature, θ_c , for copper-nickel alloys.	44
15.	Atomic susceptibility of the copper-nickel and silver-palladium systems.	47

LIST OF TABLES

Table	No. Pa	age
1.	$\Theta_{\rm R}$ (280 $^{\rm O}$ K) values for copper-nickel and copper-zinc alloys.	30
2.	Slope of the $\log(\rho-\rho_0)$ versus \log T plots for copper-nickel alloys.	50
3.	Electrical resistivity of copper-nickel and copper-zinc alloys.	31
4.	Specific heat constants for copper-nickel alloys.	48

LIST OF APPENDICES

Appendix	No.	Page
I.	Sources and chemical analyses of materials.	54
II.	Details of the melting and annealing processes.	55

I. INTRODUCTION

Although there are several methods of obtaining precise information concerning the Fermi surface in extremely pure metals, there is no direct experiment which will give this information for concentrated alloys. It is necessary to deduce information about the Fermi surface of alloys from measurements of bulk properties of the sample. Two such properties are thermoelectric power and electrical resistivity.

After reviewing the results of Schroeder and Henry (1963) concerning the thermopower of copper-zinc alloys, it was decided that a study of copper-nickel alloys might give similarly interesting results.

This thesis (1) describes the construction of an apparatus for the measurement of both thermopower and electrical resistivity of copper-nickel alloys from 4.2° to 300° K, (2) describes the procedure used in making the alloy samples, and (3) presents an analysis of the data.

II. THEORY

A. Thermoelectric Power

1. <u>Diffusion thermopower</u>. If, in the derivation of thermopower, we take account of the scattering processes but neglect the effect of the net phonon drift velocity, then we arrive at an expression for the diffusion thermopower of a material.

Mott and Jones (1936) state that the diffusion component of the thermopower of a material is

S (diffusion) =
$$\frac{\pi^2}{3} \frac{K^2T}{e} \left\{ \frac{\partial}{\partial E} [\log \sigma(E)] \right\}_{E=r}$$

where $\sigma(E)$ is the electrical conductivity of the material and η is the Fermi energy. The above expression holds at low temperatures if impurity scattering predominates and at high temperatures $(T > \Theta)$.

If the phonons have a net drift velocity, which is always the case when there is a temperature gradient in the material, then they will interact with the electrons and thereby affect the thermopower. The change in thermopower due to this interaction is called the phonon drag contribution to the thermopower. The total thermopower of a material is the sum of the diffusion and phonon drag components.

Gold et al. (1960) suggest that, under certain conditions, it is possible to separate the impurity scattering and thermal scattering components of the diffusion thermopower. In the case of dilute alloys containing two or more scattering mechanisms which are independent of each other, the total diffusion thermopower can be expressed by the Kohler relation

$$S(diff.) = \frac{\sum_{i} W_{i}S_{i}}{\sum_{i} W_{i}}$$

where $W_i(T)$ and $S_i(T)$ are the thermal resistivity and characteristic thermoelectric power (at temperature T) of the i^{th} scattering mechanism.

Assuming that the thermal resistivities \textbf{W}_{i} and electrical resistivities, $\rho_{\text{i}},$ are related by the Wiedemann-Franz Law

$$W_{i} = \frac{\rho_{i}}{L_{O}T}$$

where $L_0 = \frac{\pi^2 K^2}{3e^2}$, then the above equation can be written

in the form of the Nordheim-Gorter relationship

$$S(diff) = \frac{\Sigma \rho_i S_i}{\Sigma \rho_i}.$$

For the case of copper-nickel alloys, this relationship becomes

$$S(diff) = \frac{\rho_{Ni}S_{Ni}}{\rho} + \frac{\rho_{Th}S_{Th}}{\rho}$$
$$= S_{Ni} + \frac{\rho_{Th}}{\rho}(S_{Th} - S_{Ni})$$

where $\rho=\rho_{\rm Ni}+\rho_{\rm Th}$, $S_{\rm Ni}(T)$ and $S_{\rm Th}(T)$ are the characteristic thermopowers at temperature T due to the nickel and thermal scattering mechanisms, and $\rho_{\rm Ni}$ and $\rho_{\rm Th}$ are the electrical resistivities due to nickel and thermal scattering.

Since $S_{Ni}(T)$, $S_{Th}(T)$, and ρ_{Th} are constants (at a given temperature), and since $\rho = \rho_{Th} + \rho_{Ni}$ could be expected to vary linearly with concentration, a plot of S(diff) versus $\frac{1}{\rho}$ would be expected to give a straight line with the intercept on the S(diff.) axis equal to S_{Ni} .

2. Phonon drag contribution to thermopower. For the sake of simplicity, let us assume that the energy contained in the vibrating lattice is in the form of quantized "packets" of energy which we will call phonons. Our problem now is to determine the manner in which the phononelectron interactions will affect the thermopower.

At very low temperatures ($< 5^{\circ}$ K) we can assume, according to MacDonald (1962), that the number of phononelectron interactions will be much greater than the number of phonon-phonon interactions and that only one type of phonon-electron collision (normal) takes place.

MacDonald suggests that, under these conditions, the phonons may be compared to the molecules of an ideal gas; that is, a phonon energy density U(T) will exert a pressure

$$p = -\frac{1}{3} U(T)$$

on the conduction electrons. If a temperature gradient $\frac{dT}{dx}$ is present then there will be a pressure gradient $\frac{dp}{dx}$, giving rise to a net force per unit volume

$$F_{x} = -\frac{dp}{dx} = -\frac{1}{3}\frac{dU}{dx} = -\frac{1}{3}\frac{dU}{dT}\frac{dT}{dx} = -\frac{1}{3}C_{g}\frac{dT}{dx}$$

on the conduction electrons. Here, $c_{\underline{g}}=\frac{dU}{dT}$ is defined as the lattice specific heat.

This force on the conduction electrons will give rise to an electric current which is proportional to, but in the opposite direction from, the temperature gradient. This contribution to the total current is called the phonon drag current.

If an electric field $\mathbf{E}_{\mathbf{x}}$ is placed across the conductor so that no phonon drag current is allowed to flow, then we can say

$$NeE_{x} = -F_{x} = \frac{1}{3} Ce \frac{dT}{dx}$$

where N is the number of conduction electrons per unit volume.

Therefore, the phonon drag contribution to the thermopower can be written

$$Sg = \frac{E_x}{dT/dx} = \frac{Cg}{JNe}.$$

The preceding derivation assumes that only one type (normal) of phonon-electron collision occurs. However, a different type (Umklapp) of phonon-electron collision must also be taken into account. The two types of collisions are discussed below.

In the normal type interaction, the change in the electron wave vector \underline{K} is just equal to the wave vector \underline{q} of the phonon which is emitted or absorbed (see Fig. 1). That is, the normal process conserves not only energy

$$E_K' - E_K = \pm h C_S \underline{q}$$

but also momentum

$$\underline{K}' - \underline{K} = \pm \underline{q}$$
.

Here, $E_{K} = \frac{h^{2}K^{2}}{2m^{*}}$ and C_{S} is the speed of sound in the material.

Dekker (1957) points out that since the energy of the phonon is ~0.01 e.v. and the energy of the electrons on the Fermi surface is ~ several e.v., we can conclude that the energy of the electron will remain (nearly) constant even though it may be scattered through a large angle; that is, scattering occurs between points on (approximately) the same Fermi surface.

The situation shown in Figure 1 is one in which a phonon having wave vector <u>q</u> is traveling (roughly) from left to right. This corresponds to the physical situation in which the left end of the lattice is hotter than the right end, thus giving the phonons a net drift velocity to the right. A collision of the type shown in Figure 1 results in the electron gaining momentum* in the +x direction (to the right), thereby making the cold (right) end more negative.

This small increase in the momentum of the electron results in a small negative contribution to the thermopower.

The second type of phonon-electron interaction is known as the Umklapp process. In this interaction, the electron wave vector, \underline{K} , is not conserved. The momentum equation for the Umklapp process is (see Figure 2)

$$K - K' = \pm q + g$$

where \underline{g} is a reciprocal lattice vector.

In the Umklapp collision shown in Figure 2, both the electron and phonon are going (roughly) to the right (again, toward the cold end of the lattice) before the collision, but the interaction changes the direction of the electron, sending it to the left (toward the warm end).

This is not as obvious as it seems at first since m* may change during the interaction.

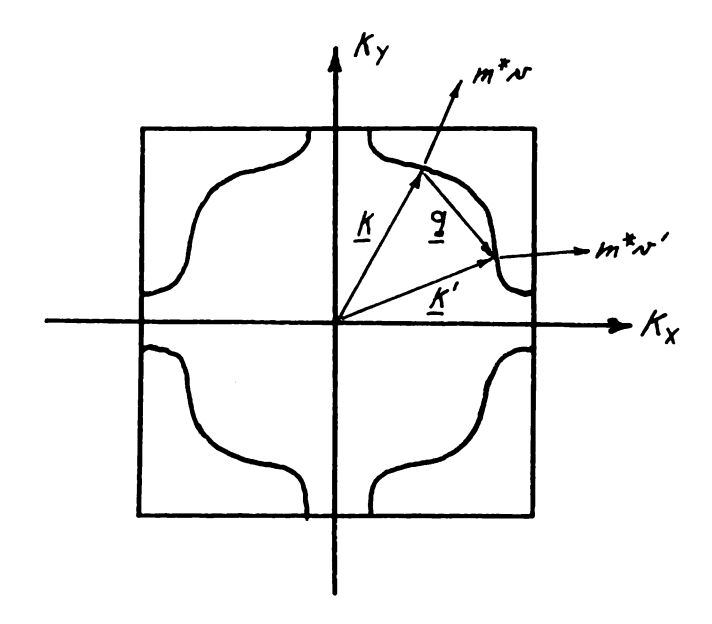


Figure 1: Normal phonon-electron interaction (Schematic)

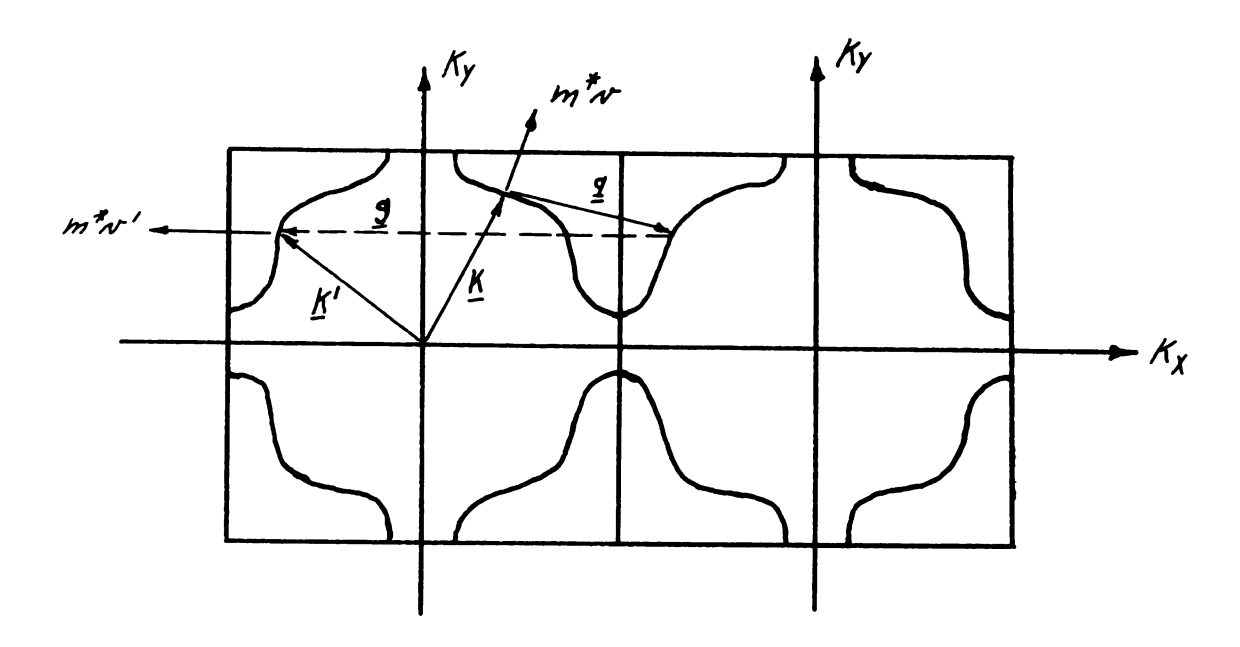


Figure 2: Umklapp phonon-electron interaction (Schematic)

This large change in the momentum of the electron and the reversal of its sign results in a large positive contribution to the thermopower.

We have found that Sg (normal) and Sg (Umklapp) give contributions of differing magnitudes and signs to S g(total). The problem is further complicated by the fact that, except at extremely low temperatures, phononimpurity scattering and phonon-phonon scattering is also important.

MacDonald suggests that all of these effects can be accounted for reasonably well if we modify our simple low temperature expression for Sg to take account of the relaxation times of the various processes.

$$Sg = \frac{Cg}{\sqrt{Ne}} \frac{\tau_o}{\tau_o + \tau_{pe}}$$

where τ_{pe} is the relaxation time for phonon-electron interactions and τ_{o} is the relaxation time for all other interactions.

At relatively high temperatures, $T>\theta_D$, the expression for Sg can be analyzed as follows: Since τ_{pe} is approximately constant and is much larger than τ_{o} , and since $\tau_{o} \propto \frac{1}{T},$ we can say

Sg
$$\propto \frac{\tau_0}{\tau_{pe}} \propto \frac{1}{T}$$
 for $T > \theta_D$.

This suggests that Sg decreases as $\frac{1}{T}$ at higher temperatures, which is roughly correct. However, it gives a numerical result of several $\mu v/^{O}K$ at room temperature, whereas experiments show that Sg \approx 0 at room temperature. MacDonald resolves this discrepancy by assuming that the normal and Umklapp processes cancel each other out at higher temperatures.

B. Electrical Resistivity

l. Characteristic temperature, Θ_R . The variation of electrical resistance with temperature is given by the Bloch-Grüneisen formula as

$$R = K \frac{T}{e_R^2} G(\frac{\theta_R}{T})$$

where G is a universal function of T having the properties that G goes to 1 as T goes to ∞ , and G goes to 497.6 $(\frac{T^4}{e_R^4})$ as T goes to 0. Θ_R is the associated characteristic temperature and K is the phonon-electron interaction constant. The Bloch-Grüneisen formula is valid only for pure metals since it assumes that the Debye Model of specific heat is valid.

Since K can be neither calculated nor measured very accurately, it is necessary to eliminate it before θ_R can be calculated. If we follow method 3 given by Kelly and

MacDonald (1953) and assume that $\theta_{\rm R}$ is constant, then we can differentiate the Bloch-Grüneisen formula to obtain

$$\frac{dR/dT}{R/T} = 1 + \frac{d \log G}{d \log \left(\frac{R}{T}\right)}.$$

Kelly and MacDonald calculate the value of the right hand side of this equation and plot it against $\frac{\Theta_R}{T}$. From this graph, one can easily find the value of Θ_R corresponding to any experimentally found value of $\frac{dR/dT}{R/T}$.

2. Temperature dependence of the electrical resistivity. In the limits of very high and very low temperatures, the Bloch-Grüneisen formula becomes

$$R \longrightarrow (\frac{K}{\Theta_R^2})T \quad \text{as} \quad T \longrightarrow \infty$$

$$R \longrightarrow (\frac{K}{e_R^6})T^5$$
 as $T \longrightarrow 0^0 K$

Assuming that K and θ_R are constants, we would expect R to be directly proportional to T at high temperatures and proportional to \mathtt{T}^5 at low temperatures.

Note that the low temperature formula is extremely sensitive to any variation in $\boldsymbol{\theta}_R$ since it contains $\boldsymbol{\theta}_R^6.$ Also, the assumption that K is constant at low temperatures is doubtful.

III. EXPERIMENTAL PROCEDURE

The work accomplished on this program can be divided into four general areas:

- A. Production of alloy samples.
- B. Construction of cryostat.
- C. Measurement of thermoelectric voltage and resistivity.
- D. Analysis of the data.

The first three of these areas will be discussed below:

A. Production of Alloy Samples.

1. <u>Production of alloys</u>. The alloys were produced by melting weighed amounts of copper and nickel in an induction furnace under a vacuum of 10⁻³ mm of mercury or better.

Two of the alloys (0.85% and 17.10% nickel) were melted in a vycor crucible while the third (3.45% nickel) was made in an alumina crucible. The pure copper sample could be made directly from the copper rod without melting. Graphite was not a suitable crucible material because

The sources and chemical analyses of materials are given in Appendix I.

nickel forms a carbide. In general, the two types of crucibles worked equally well although the vycor crucibles sometimes broke while heating.

After the copper and nickel were outgassed and melted under vacuum, the alloy was chill cast by pouring it into a heavy copper mold having a cavity about one inch deep by three-eighths inch in diameter. These castings were remelted in the induction furnace and re-poured (this time into a mold about one-quarter inch in diameter) in order to produce more homogeneous alloys.

2. Production of wires. Wires on the order of one meter long by 0.02 centimeter in diameter were produced by rolling the above mentioned castings into rod-like forms about one-eighth inch in diameter and pulling these rods through a series of about thirty steel and diamond dies. The wires were etched lightly in nitric acid after every third die to remove surface impurities.

The resistivity sample wire was wound on its vycor rod (about two inches long by one-quarter inch in diameter) and both sample wires were placed in a one-half inch diameter vycor tube which was then evacuated and sealed. This tube was placed in a platinum wound furnace and the alloys were annealed and cooled slowly to room temperature.

Details of the melting and annealing procedures are given in Appendix II.

B. Construction of Cryostat.

The cryostat was designed so that the thermoelectric voltage and resistivity of an alloy could be measured simultaneously from 4.2°K to 300°K. The high cost of liquid helium and the relatively long time required for the helium run (about 8 hours) required that heat leaks into the system by kept to a minimum.

Basically, the cryostat (see Fig. 3) consists of a double-dewar in which is suspended an insulated copper block containing most of the important elements (thermo-meter, sample junction, heater) of the system. The copper block, which can be electrically heated, has a thin-walled stainless steel tube attached to it and extending down into the liquid helium or nitrogen. This copper block and its stainless steel tail is called the sample holder.

1. Design of the sample holder. The cryostat was designed around a copper block (see Fig. 4) containing inserts for the resistivity sample, platinum resistance thermometer, carbon resistance thermometer, and the hot junction of the thermoelectric voltage sample. Other important features of the block are (1) a projection around which a heater is wrapped, (2) horizontal and vertical grooves to simplify the wiring, (3) three small holes in the base through which leads may be run, and (4) a threaded base.

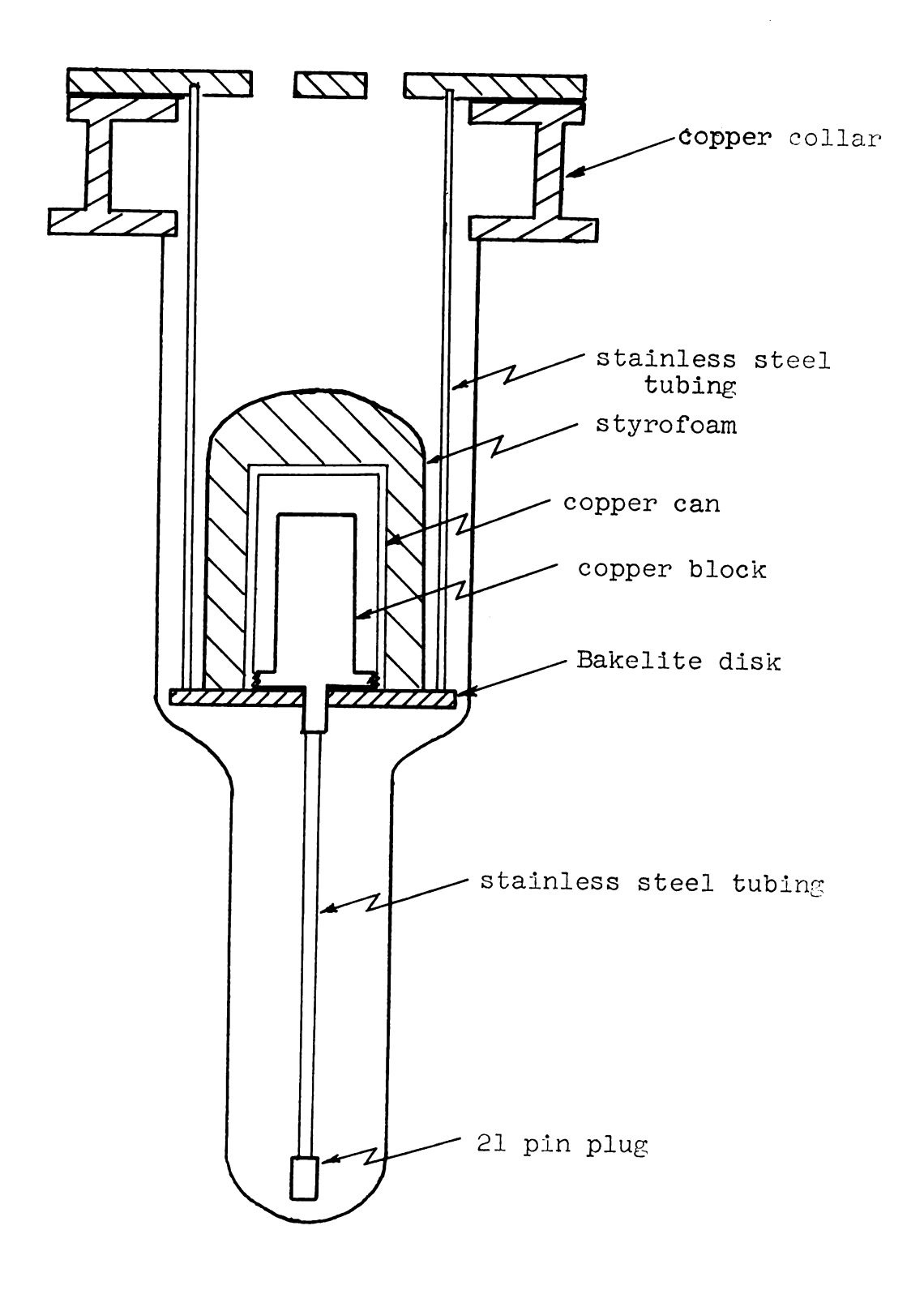


Figure 3: Cryostat

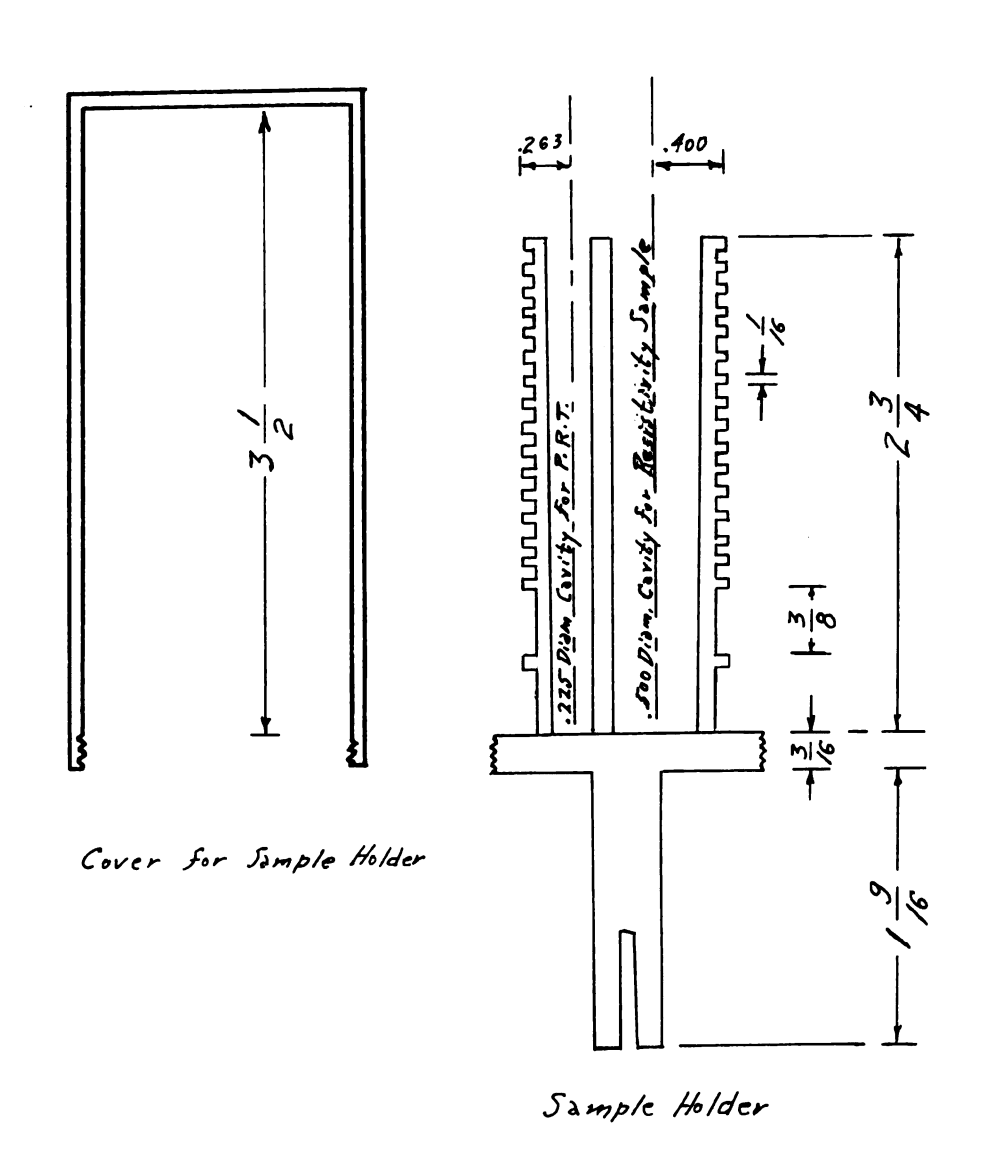


Figure 4: Copper Block

A copper "can" or cover fits over the block and screws onto its threaded base. This cover, with a one-inch thickness of styrofoam over it, provides an approximately isothermal enclosure.

Each of the electrical leads entering or leaving the enclosure is wrapped around its assigned horizontal slot six times in order to insure that the leads, copper block, and thermometers are all at the same temperature. The vertical grooves, which are deeper than the horizontal ones, are used to carry the wires from the horizontal grooves to the active elements. With this arrangement, any lead may be removed or replaced without disturbing any of the other leads.

2. <u>Wiring of the sample holder</u>. The stainless steel tube, previously called the tail of the sample holder, serves two purposes: (1) it provides a good place to attach a 21-prong plug, a resistance heater, and the cold-junction of the thermoelectric voltage sample; (2) it provides a heat leak from the copper block from and to the liquid helium or nitrogen. These two purposes will be discussed below.

It is very helpful to be able to disconnect the sample holder from the measuring circuit so that it may be taken to a workbench for the purpose of changing samples or making repairs. In order to avoid producing unwanted

thermoelectric voltages at these connections, the plug must be put into the circuit at a place where there will be no temperature gradient across it. It was convenient for us to put the plug at the bottom of the stainless steel tail where it would be covered with either liquid helium or liquid nitrogen during the entire experiment.

In the original design, all leads from the measuring circuit went into the dewar, down to the 21-prong plug, and then up (taped to the tail) to the copper block. Later, in the interest of conserving liquid helium, the leads to the top heater were brought directly into the block without going through the plug and the liquid helium.

The cold-junction of the Lead-alloy thermocouple is made at one pin of the 21-prong plug. It is interesting to note that having this arrangement eliminates the need for one of the two Lead wires in the Lead-alloy-Lead system. That is: instead of a copper-Lead-alloy-Lead-copper system, we used a copper-Lead-alloy-copper system, where the Lead wire at the cold-junction could be omitted since the entire length of it would be at 4.2° or 77°K. This arrangement is especially useful since Lead wire is soft and easily broken.

A five hundred ohm resistor attached near the bottom of the tail is used as a heater to evaporate liquid nitrogen left in the bottom of the dewar after an experiment or to

lower the level of liquid nitrogen during the experiment when necessary.

In agreement with accepted practice, the resistivity sample, platinum resistance thermometer, and carbon resistance thermometer each have two current and two voltage leads. The only other leads going into the dewar are the two copper leads to the Lead-alloy thermocouple and the two pairs of leads which supply current to the two heaters.

If the tail did not provide a heat leak from the copper block to the liquid helium or nitrogen, the block would lose heat so slowly that it would be extremely difficult to reach thermal equilibrium at temperatures near that of the cold-junction. In fact, it was found that additional heat leaks were necessary when the block was less than 30°K above the temperature of the cold-junction. The extra heat leaks were provided by hanging short lengths of No. 30 gauge copper wire from the copper block down into the tail of the dewar. The lengths of these wires were chosen so that they were long enough to reach into the liquid nitrogen or helium at the start of the experiment and short enough to be out of the liquid by the time the temperature of the block had been raised 30°K.

When the temperature difference between the copper block and cold-junction was greater than 30° , enough heat leaked down the tail so that good temperature stability was

relatively easy to maintain. We found that the temperature stability improved as the temperature of the copper block increased.

- C. Measurement of Thermoelectric Voltage and Resistivity
- 1. Design of the measuring circuit. Both the thermopower and resistivity measurements required that the temperature of the copper block be known within 0.1°K throughout the range from 4.2° to 300°K. This temperature measurement was accomplished by using a C.R.T. in the range from 4.2°K to 16° K and a P.R.T. in the range from 16° K to 300° K. Since we wanted to limit the power put into the cryostat to microwatts, it was decided that the C.R.T. ($R_{4.2} \sim 10{,}000$ ohms) current should be 10 microamps and the P.R.T. ($R_{273} \sim 30$ ohms) current should be 2 milliamps.

Using a current of 2 milliamps for the resistivity sample ($R_{273} \sim 1$ ohm) and putting the appropriate shunt across the C.R.T. enabled us to use the same current source, a six volt storage battery, for all elements (see Fig. 5). The 2 milliamp current is regulated manually with a 0-200 ohm heliopot and is monitored throughout each run by a L and N type K3 potentiometer which reads the voltage produced across a one ohm standard resistor.

 $^{^{-3}}$ C.R.T. = Carbon resistance thermometer.

P.R.T. = Platinum resistance thermometer.

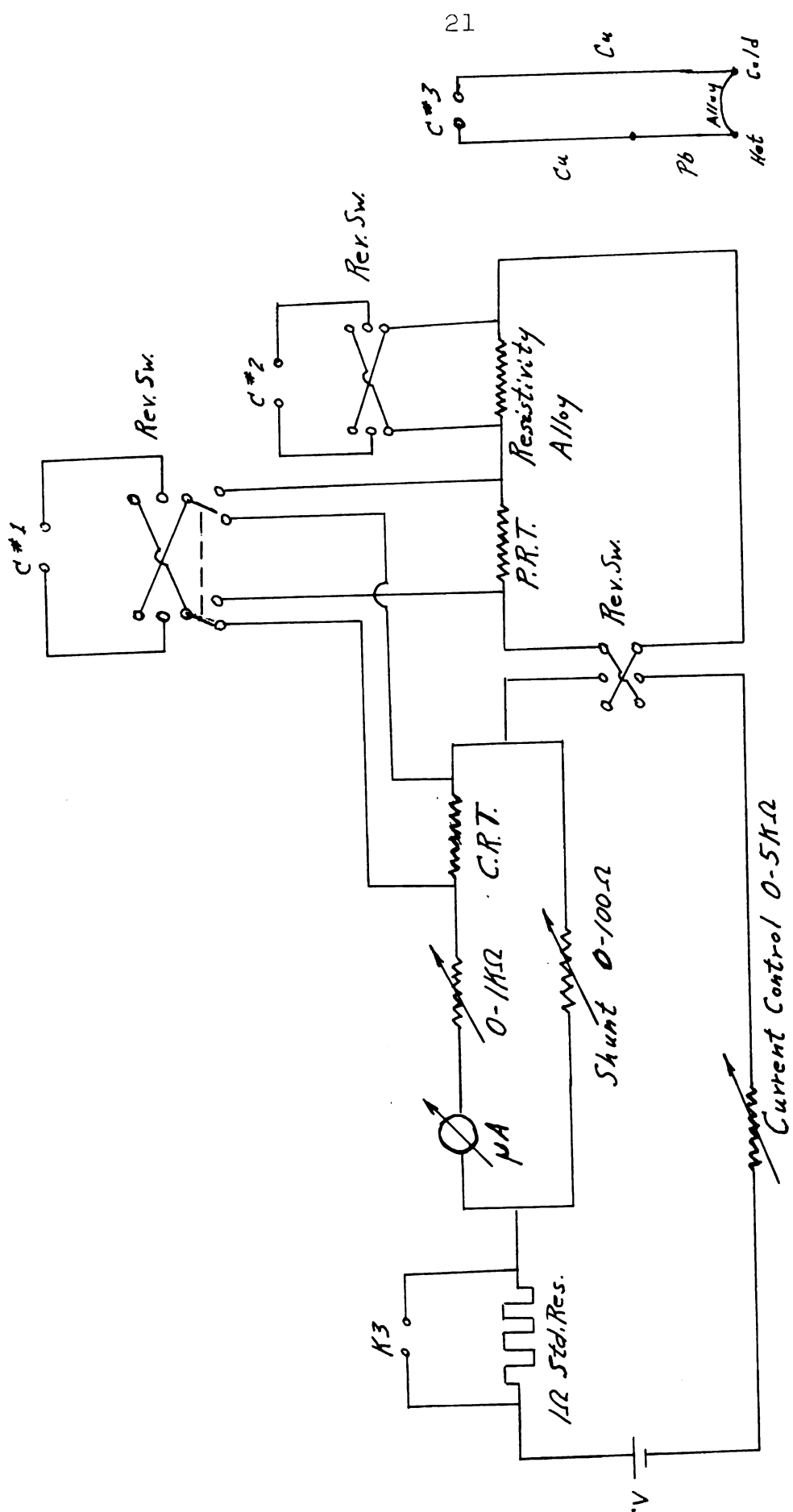


Figure 5: Electrical Circuit

Bringing the potential leads of the C.R.T. and P.R.T. to one input (No. 1) of the three-input Cambridge Microstep potentiometer used in conjunction with a photocell amplifier makes it possible to determine the temperature to within 0.1° K.

The potential leads of the resistivity sample are connected to input No. 2 of the Cambridge Microstep potentiometer. Current reversing switches are used to eliminate unwanted thermoelectric voltage from the P.R.T. and resistivity readings.

The voltage readings of the Lead-alloy thermocouple are measured on input No. 3 of the Cambridge Microstep potentiometer. A reversing switch allows for the change in sign of the thermoelectric voltage (needed only for "pure" copper), and a shorting switch is used at intervals to insure that the voltage being read is really coming from the Lead-alloy thermocouple, rather than from other sources such as the potentiometer junctions.

2. Procedure used in making measurements. The thermoelectric voltage and resistivity of each of the four sets of samples was measured from 4.2° to $\approx 100^{\circ}$ K with the cold-junction in liquid helium and from 77° to $\approx 300^{\circ}$ K with the cold junction in liquid nitrogen.

Initially, the liquid helium or nitrogen partly covered the copper block, thus insuring that both the copper block and the cold-junction were at either 4.2° or 77° K.

This provided a good preliminary check on all measurements.

The temperature of the copper block was raised in steps of 3° by putting power (controlled by a variac) into the top heater. After bringing the system to thermal equilibrium at each temperature we would make the following measurements: P.R.T.--thermoelectric voltage--P.R.T.--resistivity sample voltage--P.R.T.--C.R.T.4--P.R.T. The current was reversed after each P.R.T. and resistivity reading, and each set of readings was averaged.

 $^{^{4}}$ C.R.T. readings were taken only from $^{4}.2^{\circ}$ to 16° K.

IV. RESULTS

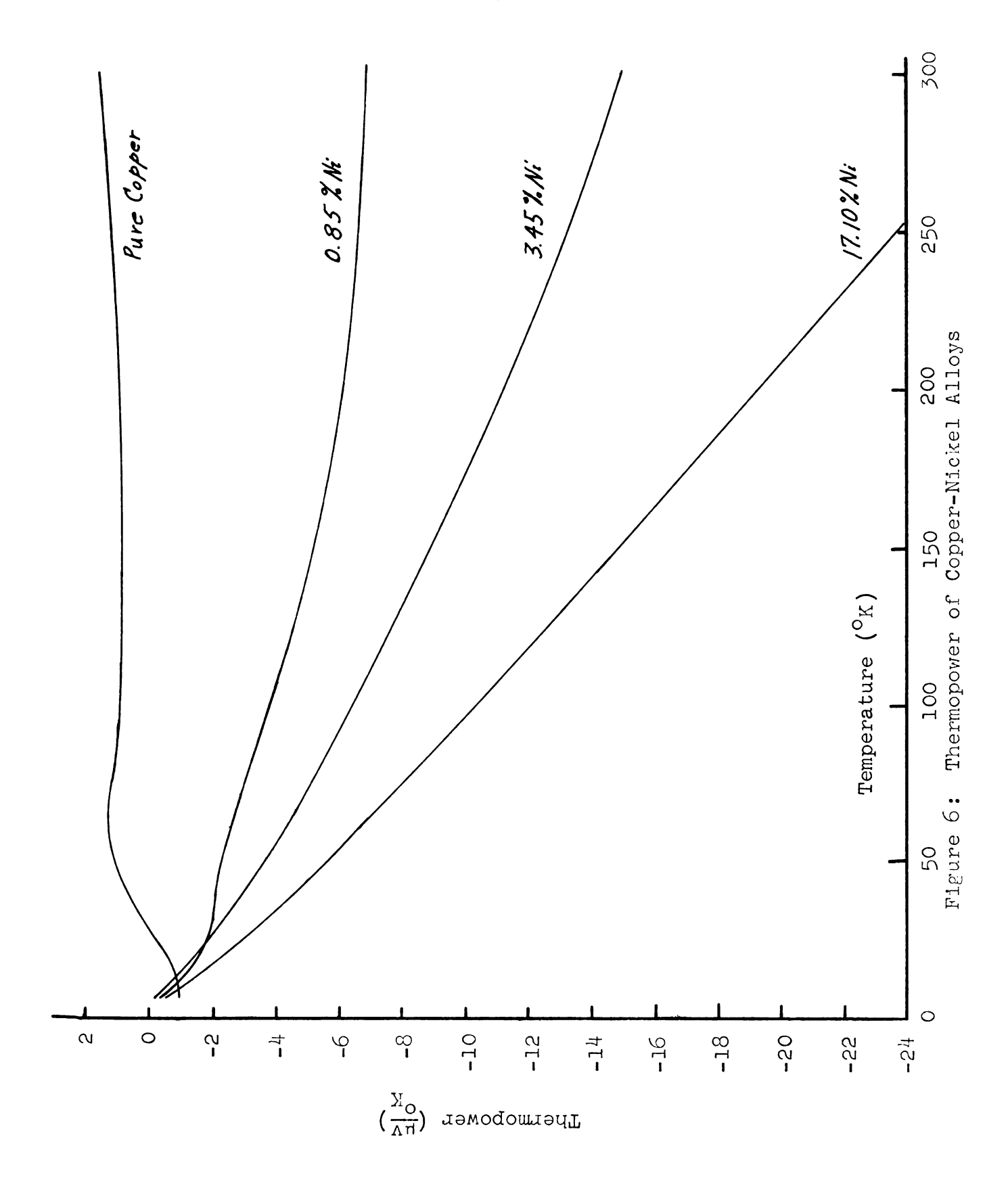
A. Thermopower

The thermopower of pure copper was found to be positive above $27^{\circ} K$ and have a local maximum of $1.25~\mu v/^{\circ} K$ at about $60^{\circ} K$. This result has been well established by other investigators [Blatt and Kropschot (1960); Gold, MacDonald, Pearson, and Templeton (1960)], and our data agrees closely with their published findings. The peak at $60^{\circ} K$ is attributed to the Umklapp phonon drag contribution.

We found that the thermopowers of the alloys were negative at all temperatures and increasingly negative with increasing concentration (see Figure 6). There appears to be a positive phonon drag contribution of about $1/2 \, \mu v/^{O} K$ at $60^{O} K$ in the 0.85% nickel sample as would be expected from the copper-zinc results. In contrast to the copper-zinc results, however, there did not appear to be any phonon drag contribution to the thermopower of either the 3.45% or 17.10% nickel sample.

B. Electrical Resistivity

1. Characteristic temperature, Θ_R . With the exception of the 17.10% nickel sample, which did not give



•

meaningful θ_R results* it was found that (1) θ_R for a given alloy is about constant or increases slightly with temperature and (2) θ_R at any given temperature decreases with concentration (see Figure 7).

Values of θ_R at $280^O K$ are given in Table 1 for both the copper-nickel alloys and the corresponding copper-zinc alloys.

2. Temperature dependence of the resistivity. The resistivity versus temperature curves for the four samples are shown in Figure 8. The resistivity was found to be approximately linear with temperature at high temperatures and (with the exception of the 17.10% nickel sample) roughly proportional to T^5 at low temperatures. The log $(\rho - \rho_0)$ versus log T curves from which the power of the temperature dependence was calculated, are shown in Figure 9. The slopes of these curves over the region of interest, 15^0 K to 30^0 K, are listed in Table 2.

Values of the residual resistivities of both the copper-nickel and copper-zinc alloys and also the resistivities of the copper-nickel alloys at 280°K are listed in Table 3.

^{*} θ_R for the 17.10% sample was 230° at 60°K, rose to a peak of 300° at 100° K, and then fell to 155° at 280° K. Since θ_R is extremely sensitive to $\frac{dR}{dT}$, the large (assumed) error in these results is probably due to a relatively small error in the resistivity versus temperature data.

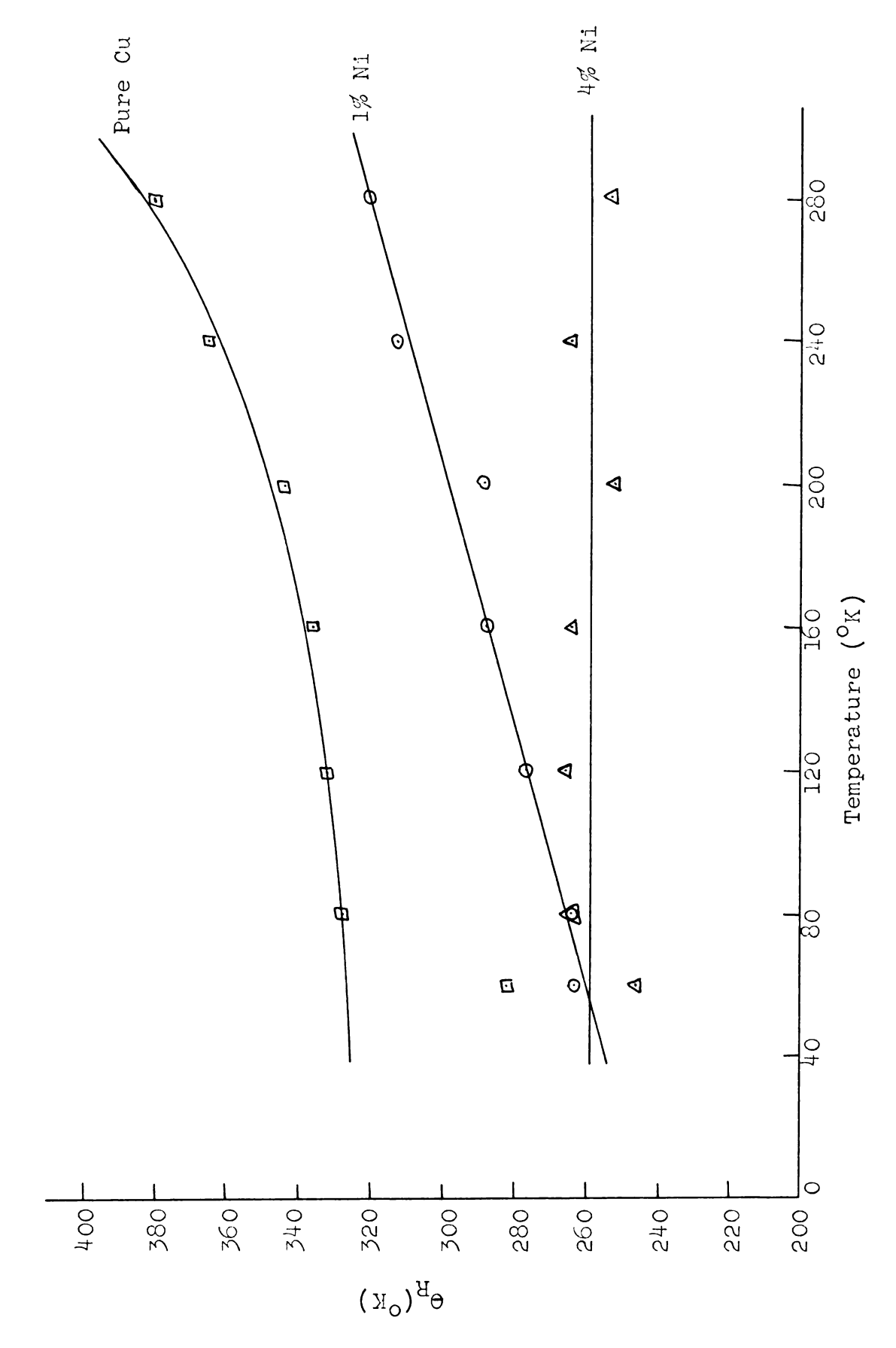


Figure 7: Characteristic Temperature, θ_{R} , of Copper-Nickel Alloys.

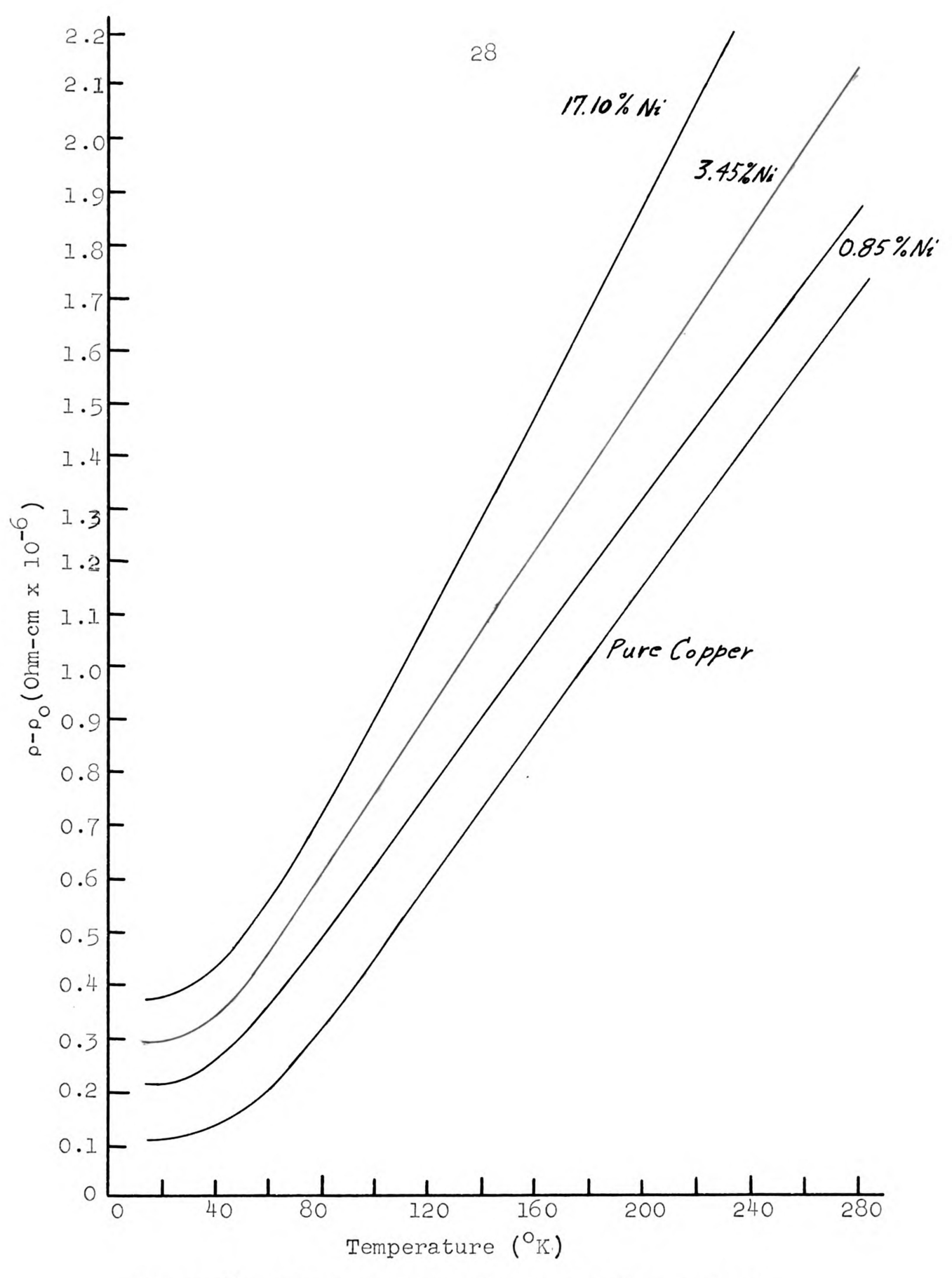


Figure 8: Ideal Resistivity versus Temperature for Copper-Nickel Alloys.

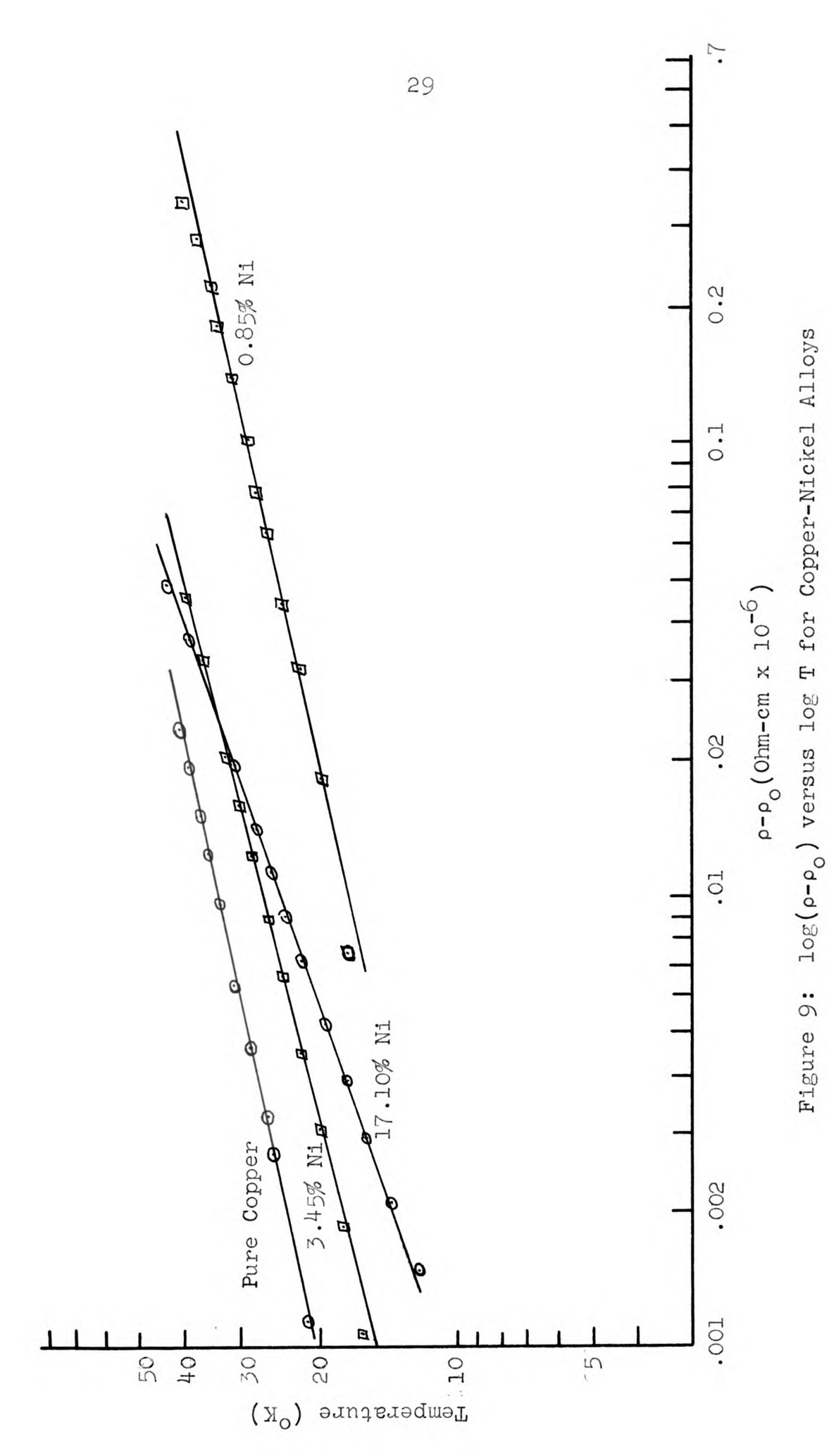


Table 1 $e_{R} \text{ (280}^{O}\text{K) values for copper-nickel}$ and copper-zinc alloys.

	$\Theta_{ m R}$ (280 $^{ m O}$ K) in $^{ m O}$ K	
Sample (% Ni or Zn)	Cu-Ni	Cu–Zn
Pure copper	380	~ 370
0.85%	321	~ 357
3.45%	273	~ 332
17.10%		~ 27 ¹ 4

Table 2 Slope of $\log(\rho-\rho_0)$ versus \log T plots for copper-nickel alloys.

Sample	Slope $(\frac{\mu \text{ Ohm-Cm}}{O_{\text{K}}})$
Pure copper	4.8 ± 0.3
0.85% Ni	4.6 ± 0.3
3.45% Ni	4.1 ± 0.3
17.10% Ni	2.9 ± 0.3

Table 3

Electrical resistivity of copper-nickel and copper-zinc alloys.

	Resistivity (µ Ohm-Cm)		
	Cu-Zn Cu-Ni		-Ni
Sample (% Ni or Zn)	ρ4.2	ρ4.2	p280
Pure Copper	0.002	0.0038	1.59
0.85%	≈ 0.225	1.06	2.70
3.45%	≈ 0.750	4.29	6.12
17.10%	≈ 2.70	19.46	21.59

From these values we find that, for "pure" copper

$$\frac{\rho 280}{\rho 4.2} = \frac{1.59}{0.0058} = 418$$

In order to determine the effect of work hardening due to wrapping the resistivity sample on the quartz rod, two identical copper samples were prepared exactly as the sample had been. One was annealed before being wrapped on its quartz rod, and the other was annealed afterwards. The residual resistivities of these test samples were found to be

$$\frac{\rho^4.2 \text{ (annealed after winding)}}{\rho^4.2 \text{ (annealed before winding)}} = (2.60)^{-1}$$

Therefore, the "true" resistivity ratio of our "pure" copper was

$$\frac{\rho 280}{\rho 4.2}$$
 = 418 x 2.60 = 1087.

This value compares favorably with the value given by Schroeder and Henry for A. S. and R. copper $(\frac{\rho 293}{\rho^4 \cdot 2} = 1316)$ after annealing in argon) and by Blatt and Kropschot $(\frac{R_{273} - R_{l_{\! 4} \cdot 2}}{R_{\! 4 \cdot 2}} = 185)$ unannealed and $(\frac{R_{273} - R_{l_{\! 4} \cdot 2}}{R_{\! 4 \cdot 2}} = 540)$ annealed).

Another interesting finding was that both the 0.85% and 3.45% samples had resistivity minimums of about 0.01×10^{-6} ohm - cm at about 13° K. Neither the pure copper nor the 17.10% sample had a resistivity minimum.

A plot of $S(280^{\circ}\text{K})$ versus $\frac{1}{\rho(280^{\circ}\text{K})}$ showed that the points for the pure copper, 0.85% nickel, and 3.45% nickel samples lay on a straight line as predicted by the Nordheim-Gorter relationship (see Figure 10). The point corresponding to the 17.10% nickel alloy was not expected to fall on the straight line since it is a concentrated alloy. Schroeder and Henry (1963) found that a similar plot for copper-zinc was linear up to 12% zinc.

The extrapolated straight line in the S versus $\frac{1}{\rho}$ graph intersected the S-axis at

$$S_{\text{Ni}}(280^{\circ}\text{K}) = -19.0 \frac{\mu\text{V}}{\circ_{\text{K}}}$$
.

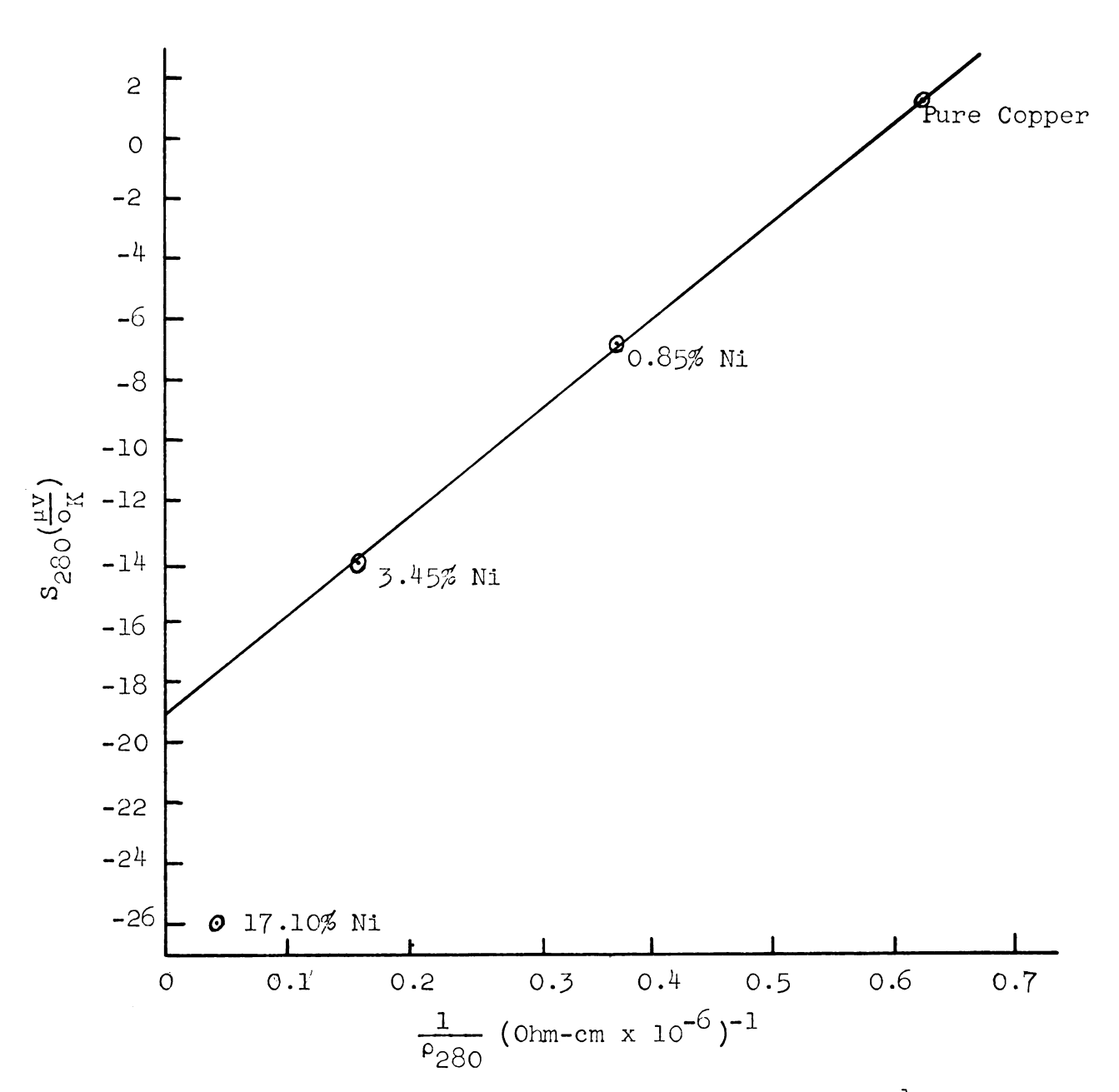


Figure 10: Thermopower (280°) versus restivity⁻¹ (280°) for Copper-Nickel Alloys

V. ANALYSIS OF RESULTS

A. Thermopower Results

1. Relation between the measured thermopower and the absolute thermopower of the alloys. Consider a simple experimental setup consisting of the sample wire A and lead wires B (see Figure 11). If we attempt to measure the thermoelectric voltage V_{54} across A due to the temperature difference T_2 - T_1 , we will actually measure the thermoelectric voltage produced by the entire system (A + B).

If A and B are the same material then, by simple conservation arguments, we must have \mathbf{V}_{34} = 0.

If A and B are different materials, we will measure

$$V_{3^{l_1}} = \int_{T_1}^{T_2} \left[\frac{dV_B}{dT} - \frac{dV_A}{dT} \right] dT$$

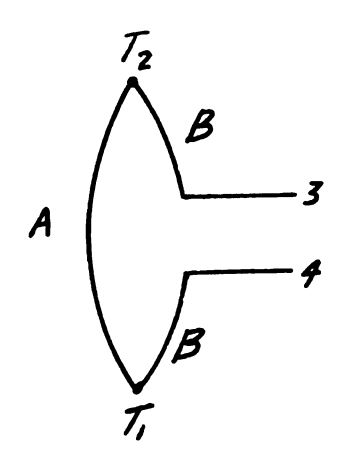
$$= \int_{T_1}^{T_2} [S_B - S_A] dT$$

so that
$$V_{34} > 0$$
 if $(S_B - S_A) > 0$
 $V_{34} < 0$ if $(S_B - S_A) < 0$.

If T_1 is kept constant then

$$S_{\text{measured}} = \frac{dV_{5/4}}{dT} = S_B J_{T_2} - S_A J_{T_2} = S_B - S_A.$$

It is obvious that either \mathbf{S}_{B} or \mathbf{S}_{A} must be known before the other can be determined. Since the absolute thermopower of Lead has been determined by Christian, et al.



$$\begin{aligned} \mathbf{V}_{3^{\frac{1}{4}}} &= \int_{\mathbf{T}_{1}}^{\mathbf{T}_{2}} \left[\frac{\mathrm{dV}_{B}}{\mathrm{dT}} - \frac{\mathrm{dV}_{A}}{\mathrm{dT}} \right] \mathrm{dT} \\ &\text{S(measured)} &= \frac{\mathrm{dV}_{3^{\frac{1}{4}}}}{\mathrm{dT}} = \mathbf{S}_{B} - \mathbf{S}_{A} \end{aligned}$$

Figure 11: Schematic Drawing of Thermopower Experiment

(1958), it was decided to use Lead lead wires to our thermopower samples. Therefore,

$$S(A) = S(B) - S(measured)$$

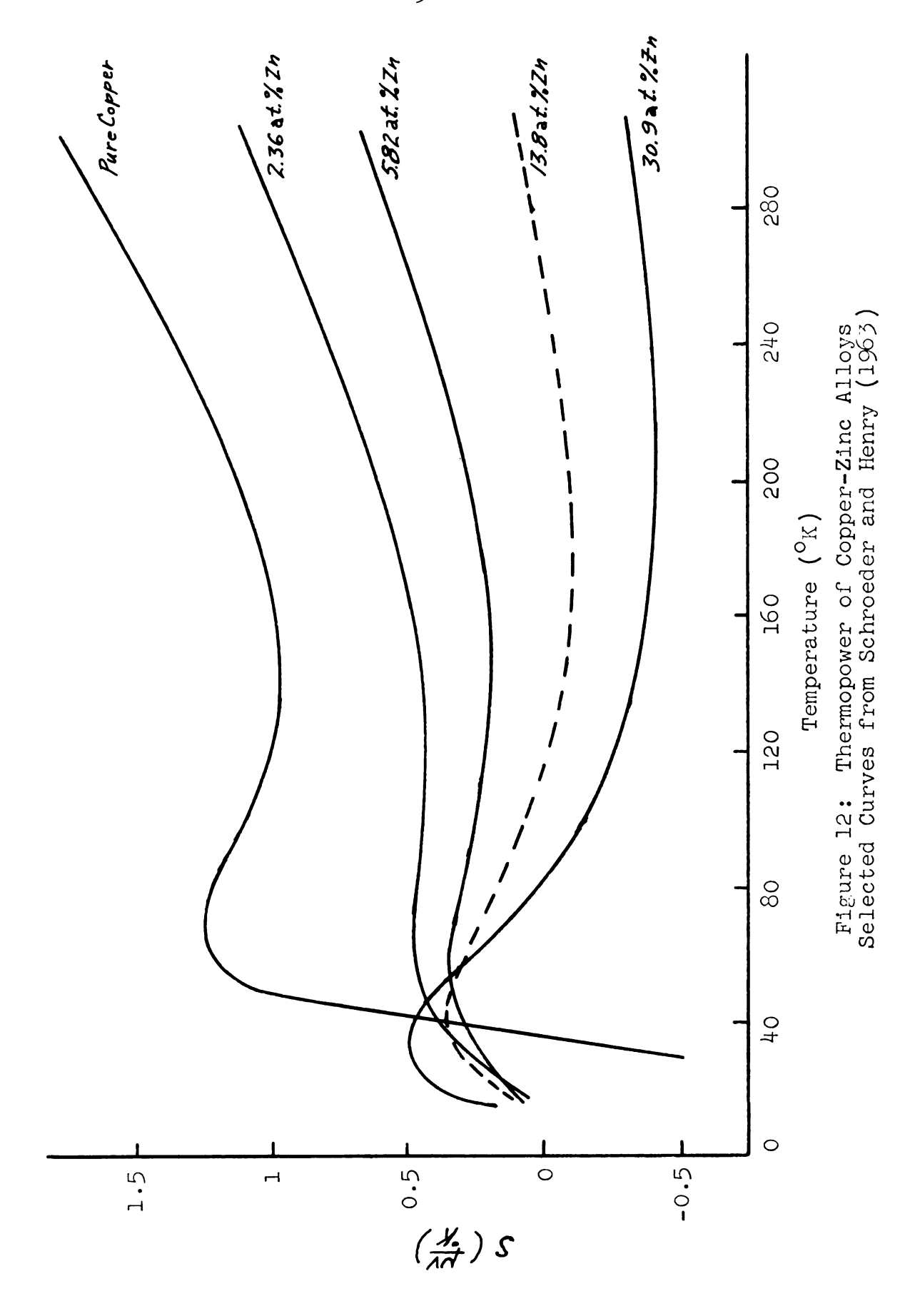
becomes

It is interesting to note that S(Lead) is negative at all temperatures while S(copper) is positive except below 20°K . We found that S(alloy) was always negative for our copper-nickel alloys.

of Schroeder and Henry (1963). Since nickel and zinc are the two immediate neighbors of copper in the periodic table, it is reasonable to expect that the thermopowers of coppernickel alloys may resemble those of copper-zinc alloys. For the purposes of comparison, a short summary of the Schroeder and Henry copper-zinc results follows (see Figure 12).

Schroeder and Henry found that a positive phonon drag component of thermopower existed for all concentrations of zinc. The main features of their data were:

- (a) There exists a phonon drag peak between 10° and 80° K followed by a curve of positive curvature.
- (b). The magnitude of the peak decreases with concentration up to about 10 atomic % zinc, and then increases.
- (c) The position of the peak shifts to lower temperatures as the concentration increases.



The initial decrease in the phonon drag peak was attributed to increased scattering which gives a lower τ_o . The resurgence of the peak for concentrations higher than 10 atomic % was attributed to the approach of the Fermi surface to the $\{200\}$ face of the Brillouin Zone.

3. Expected relationship between the copper-nickel and the copper-zinc results. The degree to which the copper-nickel results should resemble the copper-zinc results depends on how closely (1) the value of τ_0 and (2) the shape of the Fermi surface in copper-nickel resembles the same quantities in copper-zinc.

The three main factors which affect the impurity scattering, and therefore, $\tau_{_{\rm O}},$ are:

- (a) Mass of the impurity atom: Since nickel, copper, and zinc have atomic numbers of 28, 29, and 30, respectively, we can say that $M(Ni) \approx M(Zn)$ and, therefore, nickel atoms should give about the same amount of scattering as those of zinc.
- (b) Distortion of the lattice: It has been found that nickel atoms distort the lattice less than zinc atoms. This would lead to less scattering and, therefore, to higher $\tau_{_{\rm O}}$ and higher Sg for nickel than for zinc.
- (c) Inter-atomic forces: The inter-atomic forces of copper-nickel are approximately equal to those of copper-

zinc since θ_D (Cu - Ni) $\approx \theta_D$ (Cu - Zn) as shown by Guthrie, et al. (1963) and Rayne (1957).

Each of the factors listed above indicate that $\tau_{_{\rm O}}$, and therefore Sg, should be at least as large in coppernickel alloys as it was in copper-zinc. Therefore, we would expect phonon drag peaks in copper-nickel alloys to be very prominent for all of our samples.

The other factor having an important effect on Sg is the shape of the Fermi surface. If we assume that the holes in the unfilled 3d band of nickel take free electrons away from copper atoms (when nickel is added to copper) then the energy of the copper atoms is reduced—that is, the Fermi energy of a copper—nickel alloy decreases as nickel is added. Therefore, we can say that the Fermi surface should shrink and pull away from the Brillouin Zone as the concentration of nickel is increased. This process would produce a situation highly favorable to Umklapp interactions giving large changes in electron momentum (see Figure 13) which, in turn, would produce a large positive phonon drag contribution.

It would seem, then, that any changes in either τ_{o} or the shape of the Fermi surface would be such that the phonon drag peak in copper-nickel would be greater than that in the corresponding copper-zinc alloy.

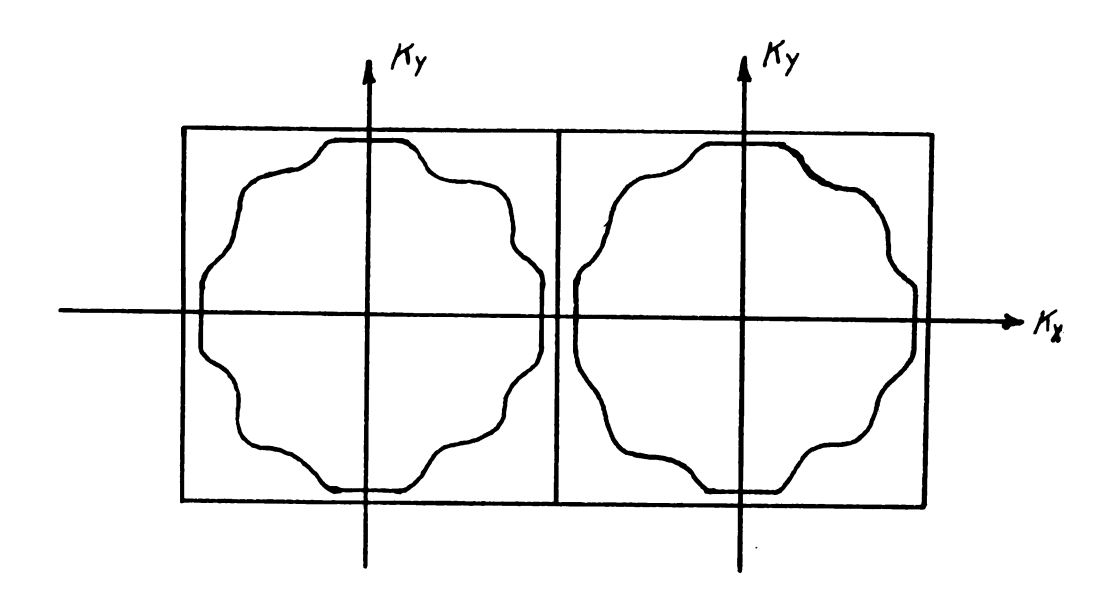


Figure 13: Fermi Surface which has pulled away from the Brillouin Zone boundary (Schematic).

4. Discussion of copper-nickel thermopower results. A comparison of the copper-nickel and copper-zinc thermopower results shows two striking differences: (1) Copper-nickel alloys have large negative diffusion thermopower, while those of copper-zinc are small for all concentrations, and positive for concentration less than 8% zinc. (2) Only the 0.85% nickel alloy showed a phonon drag component of thermopower, while all of the copper-zinc alloys showed phonon drag peaks.

What are the possible causes of these large differences? As discussed in the preceding section, they cannot be attributed to changes in τ_0 or the shape of the Fermi surface, since a change in either would be expected to increase the positive phonon drag contribution. Hopefully, any explanation of the thermopower differences would also explain the fact that nickel atoms in copper increase the resistivity much more than an equal number of zinc atoms.

One place to look for a possible explanation is the electronic structure of the nickel and zinc atoms. The outer electron configuration of atomic nickel is $3d^{8}4s^{2}$ while that of zinc is $3d^{10}4s^{2}$. The most striking difference in the configurations is that nickel has vacancies or "holes" in the 3d-band while zinc does not.

It is reasonable to assume that if the holes in the 3d-band of nickel are not filled when it is alloyed with

copper, then many of the 4s electrons from copper atoms would undergo collisions with phonons and be scattered into these empty energy states (s-d scattering). This would (1) "use up" many of the phonons so that they could not contribute to the phonon drag peak, and (2) lower the mean free path of the conduction electrons, thus increasing the resistivity.

At first glance, it would seem highly improbable that there would be any 3d-band holes unfilled in alloys having as little as 4% nickel. As pointed out by Coles (1952), the most important experimental evidence to support the belief that the 3d-band holes of copper-nickel alloys are filled for nickel concentrations of less than 40 atomic per cent is provided by a study of the ferromagnetic properties of these alloys. Both the saturation magnetic moments, $\sigma,$ and Curie temperatures, $\boldsymbol{\theta}_{C},$ of copper-nickel alloys decrease linearly with copper concentration and extrapolate to zero at 60% copper (see Figure 14). It should be remembered, however, that there are two conditions which must be satisfied in order to have a ferromagnetic material: (1) buried vacancies in the d-band and (2) correct lattice spacing. It is possible that the disappearance of ferromagnetism above 60% copper is due to the second, rather than the first, of these reasons.

Coles goes on to say that there is a great deal of experimental evidence which can only be explained by

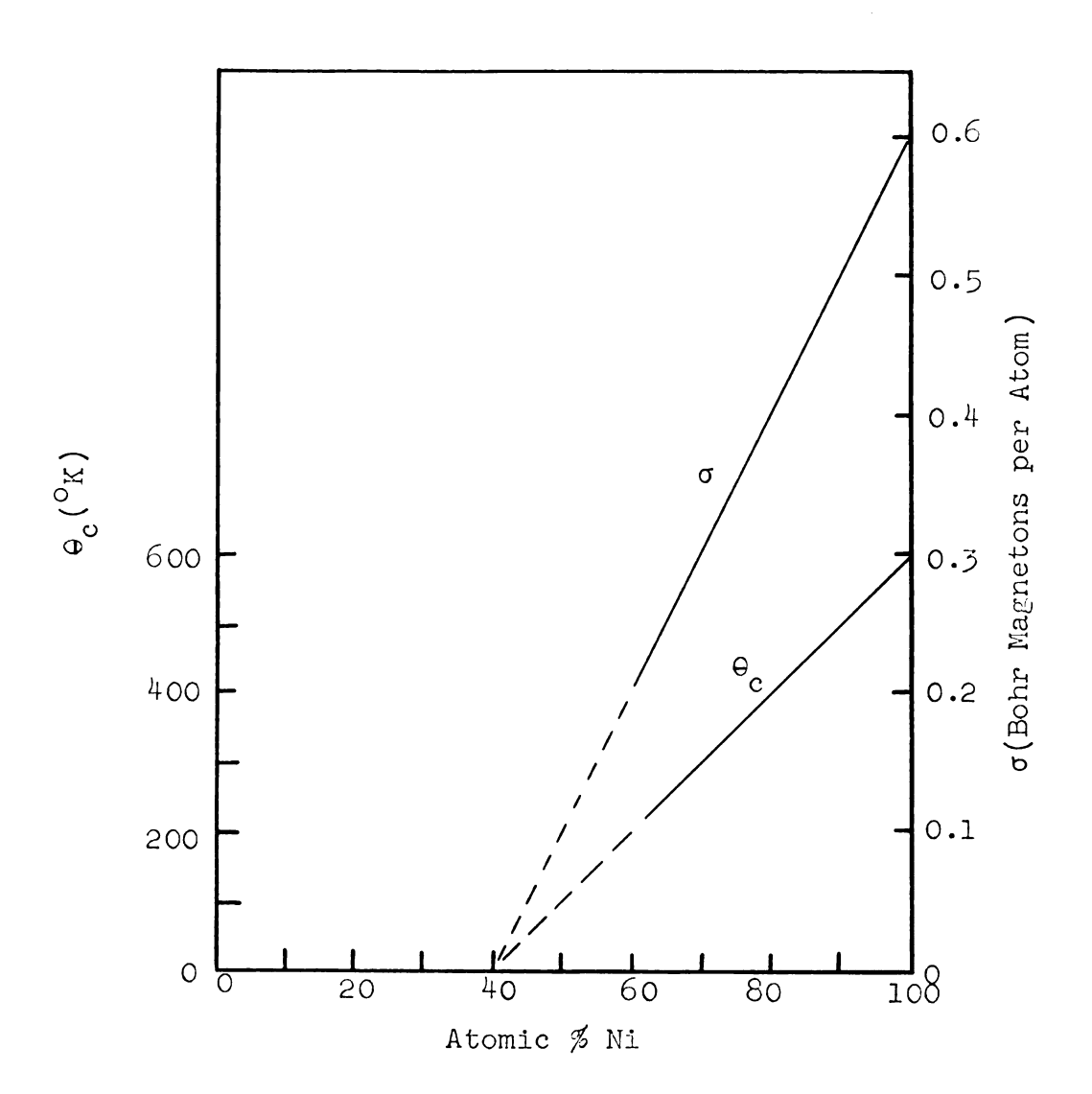


Figure 14: Saturation Magnetic Moment, σ , and Curie Temperature, θ_c , for Copper-Nickel Alloys. From Coles (1952)

assuming that 3d-band holes exist in copper-nickel alloys having concentrations as low as 3% nickel.

The most striking evidence that 3d-band holes exist down to the very low concentration of nickel comes from an examination of the paramagnetic properties of copper-nickel alloys. We know that the presence of d-band holes in non-ferromagnetic materials is indicated by high paramagnetic susceptibilities, roughly inversely proportional to temperature at high temperatures. When all the d-band states are occupied, diamagnetism is expected; the weak temperature independent paramagnetism of the conduction electrons being insufficient to overcome the diamagnetism of the full inner shells.

In order to get a clear example of how well some experimental results agree with this theory, it is instructive to look at the silver-palladium alloy system. Silver-palladium resembles the copper-nickel system in that (1) palladium precedes silver in the periodic table just as nickel precedes copper; (2) silver and copper have "similar" electronic structures--3d¹⁰4s¹ and 4d¹⁰5s¹, respectively; (3) palladium and nickel both have closed "outer" shells, namely 4d¹⁰ and 3d⁸4s², respectively; (4) all four of the elements are face centered cubic; and (5) both alloy systems show complete solid solubility.

The room temperature magnetic susceptibility of silver-palladium alloys shows exactly the behavior to be expected if all the d-band holes have disappeared when a silver concentration of about 60% silver has been reached (see Figure 15). The atomic susceptibility of coppernickel alloys, however, is quite different. The susceptibility is negative only up to about 3% nickel and is increasingly positive for higher concentrations of nickel (see Figure 15). This strongly suggests that 3d-band holes exist for concentration as low as 3% nickel, and possibly lower.

Another indication that the 3d-band holes are vacant at relatively low concentrations of nickel is given by the electronic specific heat. This specific heat can be expressed as $C_e = \gamma T$ where γ is proportional to the density of energy states at the Fermi surface. The high density of states in the unfilled 3d-band gives transition metals a high specific heat (compared to that of copper). The values found for the specific heat of various copper-nickel alloys shows that C_e goes from a low of ~ 0.2 for pure copper to ~ 0.5 for 22% nickel and levels off at ~ 1.7 (units of 10^3 cal/deg²/mol) for concentrations above 40% nickel. This suggests that the Fermi surface is in the 3d-band for 22% nickel, and, therefore, vacancies may exist at this concentration. There is no data between pure copper and 22% nickel (see Table 4).

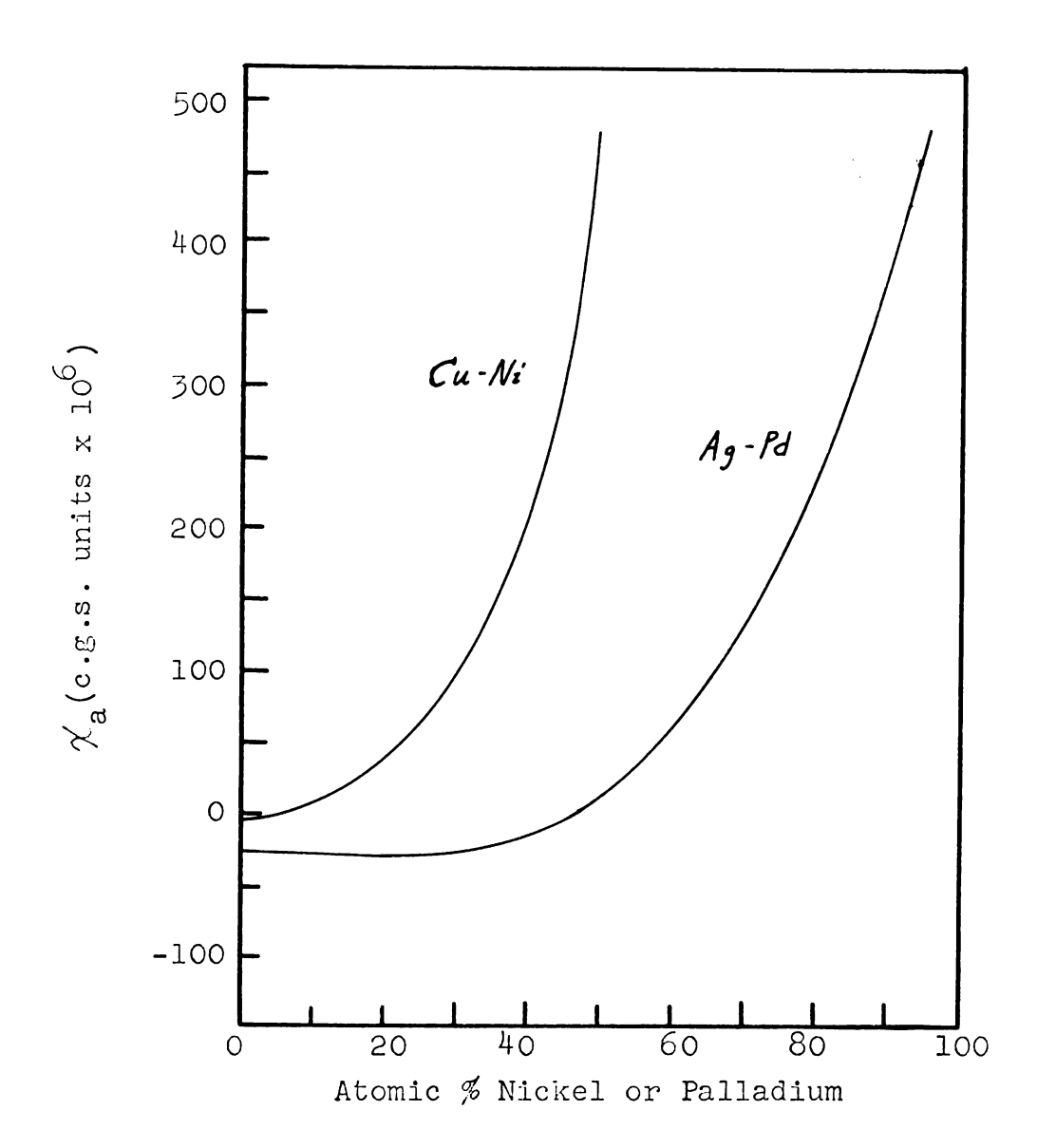


Figure 15: Atomic Susceptibility of the Copper-Nickel and Silver-Palladium Systems. From Coles (1952)

Table 4
Specific Heat Constants for Copper-Nickel Alloys
From Coles (1952)

% Nickel	$\gamma(10^3 \text{ cal/deg}^2/\text{mol})$
100.0	1.74
81.61	1.58
61.97	1.52
42.07	1.66
21.58	0.457
0	0.178
	1

In agreement with the susceptibility and specific heat data, a comparison of the resistivity results for copper-nickel and silver-palladium also suggests the presence of unfilled 3d-band vacancies at low nickel con-The resistivity of the silver-palladium system centrations. has been shown by Mott and Jones (1936) to be due to s-s scattering over the entire range of concentration and an added component of s-d scattering in the alloys having more than 40% palladium. That is, s-d scattering was found only in the range where 4d-band vacancies were thought to exist, as expected. In contrast, the resistivity of copper-nickel alloys suggests that, if a s-d scattering component does exist, it exists over the entire range of concentration (not just above 40% nickel where the alloy is ferromagnetic).

To quote Coles (1952):

Although a simple band model and collective electron treatment are appropriate in the treatment of all available data on silver-palladium alloys, they fail entirely to account for the effects found in coppernickel alloys containing less than 40% nickel. In fact, all physical properties of copper-nickel alloys are in agreement with each other in indicating the presence of 3d-band holes in alloys having as little as $\sim 5\%$ nickel.

Although it is obvious from the experimental evidence given above that the conduction electrons "think" that there are vacancies in the 3d-band, it is extremely difficult to find a model which satisfies all of the known conditions. For instance, any conduction model which results in the

correct optical energy levels will not lead to the correct resistivity and susceptibility results. It has been suggested that even at low concentrations, nickel atoms might form a d-band of their own—that is, the energy levels of the 3d-band nickel atoms would not be modified by the copper lattice. As yet, no single model can successfully explain all of the physical properties of copper—nickel alloys.

B. Discussion of the electrical resistivity results

The resistivity of each of the four samples was found to be approximately proportional to T at high temperatures as predicted by the Bloch-Grüneisen theory. At low temperatures, however, the temperature dependence differs from the predicted T^5 . Pure copper is closest with a $T^{4.8}$ dependence, followed by 0.85% with $T^{4.6}$, 3.45% with $T^{4.1}$, and 17.10% with $T^{2.9}$. The increasing variation from T^5 with concentration is not surprising since the Bloch-Grüneisen theory is valid only for pure metals and makes several approximations. The $\sim T^3$ dependence of the 17.10% sample suggests that another temperature-dependent mechanism, other than thermal scattering, is present.

The fact that the residual resistivities of the copper-nickel alloys are significantly higher than those of the corresponding copper-zinc alloys is thought to be due to s-d scattering to the 3d-band of the nickel.

The fact that the data points on the thermopower versus resistivity $^{-1}$ plot fell on a straight line intersecting the S-axis at $-19.0\,\frac{\mu\text{V}}{\text{O}_{\text{K}}}$ is interesting for two reasons: (1) The Kohler relation, which is the basis of the derivation of the Nordheim-Gorter relation, is valid for the diffusion thermopower of an alloy. Since our data at 280°K fall on a straight line when we plot the total (rather than the diffusion) thermopower against resistivity $^{-1}$, we can conclude that the phonon-drag component of the thermopower is ≈ 0 at 280°K . This is in agreement with other published results (MacDonald, 1962). (2) The intersection of the straight line at $-19.0\,\frac{\mu\text{V}}{\text{O}_{\text{K}}}$ means, by definition, that

$$S_{Ni}(280^{\circ}K) = -19.0 \frac{\mu V}{\circ K}$$
.

Gold et al. (1960) have found that $S_{Ni}(15^{\circ}K)=-1.1\,\frac{\mu\nu}{^{\circ}K}$. If $S_{Ni}(T)$ were directly proportional to T, then we would expect that

$$S_{\text{Ni}}(280) = (\frac{280^{\circ}\text{K}}{15^{\circ}\text{K}})(-1.1\frac{\mu\text{V}}{\circ\text{K}}) = -20.5\frac{\mu\text{V}}{\circ\text{K}}$$

A comparison of our result and this predicted result shows that $S_{N_1}(\mathbf{T})$ is indeed nearly proportional to temperature.

VI. CONCLUSIONS

The thermoelectric powers and resistivities of a series of copper-nickel alloys have been measured and compared to those of copper-zinc and silver-palladium alloys.

It was noted that the large negative thermopower, lack of phonon drag peaks in all but the 0.85% thermopower results, and relatively high electrical resistivity of the sample alloys were consistent with other experimental evidence suggesting that 3d-band vacancies exist in alloys having as little as 3% nickel.

A study of the thermopower and resistivity of silverpalladium alloys would give additional insight into the results found for copper-nickel alloys and provide further information about the Fermi surface of concentrated alloys.

REFERENCES

- Blatt, F. J. and Kropschot, R. H. (1959). Phys. Rev. <u>116</u>, 617.
- Coles, B. R. (1952). Proc. Phys. Soc. London 65, 227.
- Christian, J. W., Jan, J. P., Pearson, W. B., and
 Templeton, I. M. (1958). Proc. Roy. Soc. 245, 213.
- Dekker, A. J. (1957). Solid State Physics (Prentice Hall, Inc.) p. 291.
- Gold, A. V., MacDonald, D. K. C., Pearson, W. B., and Templeton, I. M. (1960). Phil. Mag. 5, 765.
- Guthrie, Friedberg, and Goldman (1959). Phys. Rev. 113, 45.
- Kelly, F. M. and MacDonald, D. K. C. (1953). Can. J. Phys. 31, 147.
- MacDonald, D. K. C. (1962). Thermoelectricity (John Wiley and Sons) p. 91.
- Mott, N. F. and Jones, H. (1936). The Theory of the

 Properties of Metals and Alloys. (The Clarendon
 Press, Oxford). p. 310.
- Rayne, J. A. (1957). Phys. Rev. <u>108</u>, 22.
- Schroeder, P. A. and Henry, W. G. (1963). The Low Temperature Resistivities and Thermopowers of α-phase Copper-zinc Alloys. (unpublished)

 $\label{eq:Appendix I} \mbox{Sources and Chemical Analyses of Materials}$

Material	Source	Purity
copper $(\frac{3}{6}$ " diam. rod)	American Smelting and Refining Co. Grade ASARCO A-58	99.999% Pure ¹ 0.01% Silver ² "Trace" Iron ²
nickel (powder)	Johnson and Matthey Cat. No. J.M. 891	99.999% Pure ¹ 0.04% Iron ²
alumina (crucibles)	McDaniel Refractory Porcelain Co. Cat. No. AP35	99% Al ₂ 0 ₃ 1
nitric acid (used to etch wire)	Fisher Scientific Co. Cat. No. A-200	0.00002% Iron ¹
Lead (10 mil wire)	Comico Electronic MaterialsSpokane, Washington	99.9999% Pure ¹

¹Advertised purity.

²Spectrographic Testing Laboratory, Detroit 12, Michigan "Trace" = < 0.01%.

Appendix II

Details of the melting and annealing processes

Sample	Annealing time	Original wts. of Cu and Ni
Pure Cu	5 hours at 580°C	10 gm Cu
0.85% Ni*	20 hours at 740°C	9.29 gm C u 0.08 gm Ni
3.45% Ni*	26 hours at 740°C	10.05 gm Cu 0.36 gm Ni
17.10% Ni*	40 hours at 780°C	8.89 gm Cu 1.55 gm Ni

Comments:

The pure copper sample was wound on a 1/4" diameter copper rod (insulated with mylar) after annealing. All other samples were wound on a 1/4" diameter vycor rod before annealing.

All samples were cooled slowly (~ 24 hours) in the furnace.

All samples were annealed in an evacuated vycor tube.

^{*}Spectrographic Testing Laboratory; Detroit 12, Michigan.